

# Membrane Composition Affects the Reversibility of Annexin A2t Binding to Solid Supported Membranes: A QCM Study<sup>†</sup>

Michaela Ross,<sup>§</sup> Volker Gerke,<sup>#</sup> and Claudia Steinem<sup>\*‡</sup>

*Institut für Biochemie, Westfälische Wilhelms-Universität, Wilhelm-Klemm-Strasse 2, 48149 Münster, Germany, Institut für Medizinische Biochemie, Zentrum für Molekularbiologie der Entzündung (ZMBE), Westfälische Wilhelms-Universität, von-Esmarch-Strasse 56, 48149 Münster, Germany, and Institut für Analytische Chemie, Chemo-, und Biosensorik, Universität Regensburg, 93040 Regensburg, Germany*

*Received October 25, 2002; Revised Manuscript Received January 16, 2003*

**ABSTRACT:** By means of the quartz crystal microbalance (QCM) technique, we investigated the interaction of porcine heterotetrameric annexin A2t with solid supported lipid membranes. Dissociation and rate constants of annexin A2t binding to various lipid mixtures were determined as a function of  $\text{Ca}^{2+}$  concentrations in solution. In contrast to what has been observed for annexin A1, the binding affinity and kinetics of annexin A2t binding are not influenced by cholesterol. In the experimental setup chosen, the annexin A2t binding is strictly  $\text{Ca}^{2+}$ -dependent and only affected by the amount of phosphatidylserine (PS) in the membrane and the  $\text{Ca}^{2+}$  concentration in solution. By  $\text{Ca}^{2+}$ -titration experiments at constant annexin A2t concentration, we investigated the reversibility of annexin A2t adsorption and desorption. Surprisingly,  $\text{Ca}^{2+}$ -titration curves display a significant hysteresis. Protein desorption curves starting from annexin A2t bound to the membrane at 1 mM  $\text{CaCl}_2$  exhibit high cooperativity with half-maximum  $\text{Ca}^{2+}$  concentrations in the submicromolar range. However, protein adsorption curves starting from an EGTA-containing solution with soluble annexin A2t always show two inflection points upon addition of  $\text{Ca}^{2+}$  ions. These two inflection points may be indicative of two protein populations differently bound to the solid-supported membrane. The ratio of these two annexin A2t populations depends on the amount of PS molecules and cholesterol in the membrane as well as on the  $\text{Ca}^{2+}$  concentration. We propose a model discussing the results obtained in terms of two binding sites differing in their affinity due to lipid rearrangement.

Annexins are a family of proteins that bind to negatively charged phospholipids in a  $\text{Ca}^{2+}$ -dependent manner (for reviews, see refs 1 and 2). Because of their membrane-binding properties, they have been implicated in a number of membrane-associated processes, including vesicle fusion, trafficking, and ion channel formation (3–5). Besides their membrane-binding properties all annexins share a particular molecular structure, which is composed of four repeating units of 70–80 amino acids (eight repeats in the case of annexin A6), known as the annexin repeat (1, 2).

Annexin A2 is unique among the annexins in that the N-terminal domain of the protein contains a high affinity binding site for the p11 dimer, itself a member of the S100 family of  $\text{Ca}^{2+}$ -binding proteins (6). The heterotetrameric complex  $(\text{A2-p11})_2$  formed by these proteins is referred to as annexin A2 tetramer (A2t) and is the predominant form in most cells. Two distinct classes of  $\text{Ca}^{2+}$ -binding sites were discovered in annexins, which differ from the well-character-

ized EF-hands (7, 8). In annexin A2, three so-called type II sites were found in repeats 2, 3, and 4, whereas two type III sites of lower affinity were localized in the first repeat of the protein (9, 10). Annexin A2t binds  $\text{Ca}^{2+}$  ions with low affinity ( $K_{0.5} = 0.5$  mM) in the absence of phospholipids (11) accompanied by a conformational change, which leads to the exposure of a Trp-residue to a more hydrophobic environment (9, 11–14). The presence of negatively charged phospholipids greatly increases the affinity of the protein for both cation and lipid (15).  $\text{Ca}^{2+}$  concentrations for half-maximum phosphatidylserine (PS)<sup>1</sup> binding of the annexin A2 heterotetramer have been determined to be 9  $\mu\text{M}$  (15), <1  $\mu\text{M}$  (16), 1.6  $\mu\text{M}$  (11), and 15  $\mu\text{M}$  (17). These  $K_{0.5}$  values are the lowest among all annexins (1). The  $\text{Ca}^{2+}$ -dependent annexin A2t binding to PS-liposomes is also accompanied by a conformational change, although it is not clear whether the conformational change is different from (11) or the same as (18) the one induced by  $\text{Ca}^{2+}$  ions in the absence of phospholipids.

<sup>†</sup> This is a contribution from the DFG Graduate College (Grant No. 234). Support by the Deutsche Forschungsgemeinschaft to V.G. is gratefully acknowledged.

<sup>\*</sup> To whom correspondence should be addressed: Institut für Analytische Chemie, Chemo- und Biosensorik, Universität Regensburg, 93040 Regensburg, Germany. Telephone: +49 941 943 4548, Fax +49 941 943 4491. E-mail: claudia.steinem@chemie.uni-regensburg.de.

<sup>‡</sup> Universität Regensburg.

<sup>§</sup> Institut für Biochemie, Westfälische Wilhelms-Universität Münster.

<sup>#</sup> ZMBE, Westfälische Wilhelms-Universität Münster.

<sup>1</sup> Abbreviations: PS, phosphatidylserine; QCM, quartz crystal microbalance; POPC, 1-palmitoyl-2-oleoyl-*sn*-glycero-3-phosphocholine; POPS, 1-palmitoyl-2-oleoyl-*sn*-glycero-3-phosphoserine; bbPC, bovine brain L- $\alpha$ -phosphatidylcholine; bbPS, bovine brain L- $\alpha$ -phosphatidyl-L-serine; SDS, sodium dodecyl sulfate; PAGE, polyacrylamide gel electrophoresis; EGTA, ethylene glycol bis( $\beta$ -aminoethyl ether)-*N,N,N',N'*-tetraacetic acid; MLV, multilamellar vesicle; LUV, large unilamellar vesicle; TCA, trichloroacetic acid.

Several studies have been performed using liposome binding assays to characterize the binding properties of annexin A2t to negatively charged lipids (11, 12, 15, 19) and cholesterol (18, 20) in the presence of  $\text{Ca}^{2+}$  ions. However, only the  $\text{Ca}^{2+}$  concentrations required for half-maximum annexin A2t binding were determined. One major drawback of such vesicle-based assays is the fact that annexin A2t does not only bind to membranes but also induces liposome aggregation (18, 20–24). Vesicle aggregation considerably complicates data interpretation and renders estimation of binding constants more complicated (17). To obtain a complete picture of the association and dissociation processes of the complex system comprising annexin A2t,  $\text{Ca}^{2+}$  ions, and lipids we used solid supported bilayers in combination with the quartz crystal microbalance (QCM) technique (25–27). This method enabled us to quantify annexin A2t–membrane interaction as a function of  $\text{Ca}^{2+}$  and annexin A2t concentration in solution without interference from membrane aggregation. It also allowed us for the first time to investigate the reversibility of annexin A2t association and dissociation to membranes as a function of the  $\text{Ca}^{2+}$  concentration.

## MATERIALS AND METHODS

**Materials.** 1-Palmitoyl-2-oleoyl-*sn*-glycero-3-phosphocholine (POPC) and 1-palmitoyl-2-oleoyl-*sn*-glycero-3-phosphoserine (sodium salt) (POPS) were purchased from Avanti Polar Lipids (Alabaster, AL). Bovine brain type III-B L- $\alpha$ -phosphatidylcholine (bbPC), L- $\alpha$ -phosphatidyl-L-serine (bbPS), and cholesterol were obtained from Sigma-Aldrich (Steinheim, Germany). Octanethiol was from Fluka (Neu Ulm, Germany). The gold used for the working electrodes was a friendly gift from DEGUSSA (Hanau, Germany). Chromium was from Bal Tec (Balzers, Liechtenstein). The 5 MHz overtone polished AT-cut quartz crystals (plano-plano) were from KVG (Neckarbischofsheim, Germany).

**Protein Purification.** Porcine heterotetrameric annexin A2 (A2t) was purified according to Gerke and Weber (28). Protein concentration was determined using an extinction coefficient of  $\epsilon_{280} = 0.65 \text{ cm}^2 \text{ mg}^{-1}$  (28). Purity was analyzed by SDS–PAGE, and the protein bands were visualized by staining with Coomassie blue.

**Vesicle Preparation.** Vesicles composed of different lipid mixtures were prepared according to the extrusion method as described elsewhere (29) in 20 mM Tris/HCl, 0.1 M NaCl, 0.1 mM EGTA, 1 mM  $\text{NaN}_3$ , pH 7.4 resulting in large unilamellar vesicles (LUVs) with a nominal diameter of 100 nm and a final concentration of 1 mg/mL.

**Annexin Binding to Liposomes.** Binding of annexin A2t to liposomes was analyzed by a  $\text{Ca}^{2+}$ -dependent copelleting assay in 20 mM Tris/HCl, 0.1 M NaCl, 1 mM  $\text{NaN}_3$ , 1 mM  $\text{CaCl}_2$ , pH 7.4. Each reaction was carried out using 4.3  $\mu\text{g}$  of protein and 50  $\mu\text{g}$  of liposomes in a total volume of 150  $\mu\text{L}$ . The samples were incubated at room temperature for 20 min and then centrifuged for 20 min at 200000g (4 °C). The pellet was either resuspended in 10  $\mu\text{L}$  of buffer (20 mM Tris/HCl, 0.1 M NaCl, 1 mM  $\text{NaN}_3$ , 0.1 mM EGTA, pH 7.4) and analyzed by SDS–PAGE or used to study the reversibility of membrane binding. In the latter case, bound protein was extracted from the liposome pellet by adding 150  $\mu\text{L}$  of buffer containing 10 mM EGTA at room

temperature for 20 min. After incubation, the mixtures were centrifuged for 20 min at 200000g (4 °C). Protein remaining in the supernatant was precipitated by adding 300  $\mu\text{L}$  of 20% (w/v) trichloroacetic acid. After 15 min on ice, the samples were centrifuged for 15 min at 10000g (4 °C). The precipitates were washed with 2% sodium acetate in ethanol (w/v) and analyzed by SDS–PAGE together with the liposome pellets and a liposome-free control.

**Preparation of Lipid Bilayers on Gold.** Solid supported lipid bilayers composed of a first chemisorbed hydrophobic octanethiol monolayer and a second physisorbed lipid monolayer were prepared on one of the two gold electrodes (0.265  $\text{cm}^2$  each) of a 5 MHz AT-cut quartz plate as described elsewhere (29). The completeness of chemisorption was verified by impedance spectroscopy (impedance gain/phase analyzer SI 1260, Solartron Instruments, Farnborough, UK). For data evaluation, an equivalent circuit composed of a capacitance  $C_m$  representing the octanethiol monolayer in series to an Ohmic resistance  $R_e$  representing the bulk resistance and the wire connections was used. Chemisorption was considered successful, when the capacitance of the octanethiol monolayer was  $(2.0 \pm 0.2) \mu\text{F}/\text{cm}^2$ . After formation of the second physisorbed lipid layer by spreading vesicles on the hydrophobic monolayer, the quality of the solid supported bilayer was again analyzed by impedance spectroscopy using the same equivalent circuit. In this case,  $C_m$  represents the capacitance of the lipid bilayer. A successful bilayer preparation resulted in capacitance values of  $(1.1 \pm 0.2) \mu\text{F}/\text{cm}^2$ . Assuming a series connection of the capacitances of the two monolayers allows calculating the specific capacitance of the second phospholipid monolayer, which was determined to be  $(2.4 \pm 0.6) \mu\text{F}/\text{cm}^2$ . Within error, the same capacitance values were obtained for all lipid mixtures. Remaining vesicles were removed by exchanging the vesicle suspension against pure buffer.

**QCM Measurements.** The QCM setup used in the present study has already been described in more detail elsewhere (29, 30). The main part is a highly polished AT-cut quartz resonator (diameter: 14 mm, fundamental resonance frequency: 5 MHz, area of the gold electrodes: 0.265  $\text{cm}^2$ ) placed in a fluid chamber made of Teflon, exposing one side of the resonator to the aqueous solution. The fluid chamber is connected to a peristaltic pump (flow rate: 0.33–0.35 mL/min) allowing the addition of solutions from outside. The quartz oscillation is driven by an oscillator circuit (TTL SN74LS124N, Texas Instruments, Dallas, TX) and read out using a frequency counter (53181A, Hewlett-Packard, San Diego, CA) connected via RS 232 to a personal computer. The entire system is placed in a water-jacketed Faraday cage thermostated at 20 °C.

## RESULTS

**Binding of Annexin A2t to POPC/POPS and POPC/POPS/Cholesterol Membranes.** For each QCM experiment, a lipid bilayer was prepared on the gold surface of a quartz plate, and its quality was checked by impedance analysis. Different annexin A2t concentrations were added to the functionalized quartz plate, and its response was monitored. Typical time courses are depicted in Figure 1. The addition of annexin A2t to POPC/POPS (80:20) membranes in the presence of 1 mM  $\text{CaCl}_2$  results in an immediate decrease in resonance

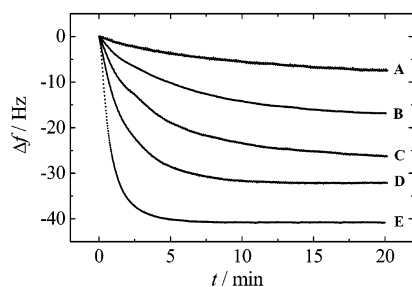


FIGURE 1: Typical time courses of frequency changes ( $\Delta f$ ) upon addition of different annexin A2t concentrations to solid supported membranes, composed of an octanethiol monolayer chemisorbed on gold, and a POPC/POPS (4:1) monolayer. The annexin A2t concentrations are: (A) 0.021  $\mu\text{M}$ , (B) 0.031  $\mu\text{M}$ , (C) 0.071  $\mu\text{M}$ , (D) 0.17  $\mu\text{M}$ , and (E) 0.43  $\mu\text{M}$ . The measurements were carried out in 20 mM Tris/HCl, 0.1 M NaCl, 1 mM  $\text{CaCl}_2$ , 1 mM  $\text{NaN}_3$ , pH 7.4.

frequency ( $\Delta f = f(t) - f_0$ ) indicative of protein adsorption to the lipid bilayer. The maximum frequency shift as well as the time required for equilibration depends on the annexin A2t concentration in solution.

Binding isotherms for a given  $\text{Ca}^{2+}$  concentration can be readily extracted from these measurements by plotting the equilibrium frequency shift  $-\Delta f_e$  vs the protein concentration in solution ( $c_{\text{AnxA2t}}$ ) assuming that the resonance frequency shift is proportional to the adsorbed protein mass (27). The binding curve is well described by a simple Langmuir adsorption isotherm (eq 1):

$$\Delta f_e(c_{\text{AnxA2t}}) = \Delta f_{\text{max}} \frac{c_{\text{AnxA2t}}}{K_d + c_{\text{AnxA2t}}} \quad (1)$$

allowing the determination of the dissociation constant  $K_d$  and the frequency shift at maximum surface coverage termed  $\Delta f_{\text{max}}$ . We are aware of the fact that an analysis of the overall binding curve as a single equilibrium process is a rather stark simplification and that a complex set of reactions is involved in the membrane binding process of annexin A2t (31–33). However, as no cooperativity was detectable when the binding curves were analyzed by Scatchard plots (data not shown) the simplification appears to be justified.

Dissociation constants for the interaction of annexin A2t to POPC/POPS (80:20) membranes were determined for three different  $\text{Ca}^{2+}$  concentrations (1, 0.1, and 0.01 mM  $\text{CaCl}_2$ ) and in the absence of  $\text{Ca}^{2+}$  ions by using a buffer without additional  $\text{CaCl}_2$  and a buffer containing 0.1 mM EGTA (Figure 2a). By fitting the parameters of eq 1 to the data the maximum frequency shift  $\Delta f_{\text{max}}$  and dissociation constant  $K_d$  of the corresponding adsorption isotherm were obtained. The values are summarized in Table 1. In 1 mM  $\text{CaCl}_2$ , a maximum frequency shift of  $-\Delta f_{\text{max}} = (42 \pm 2)$  Hz was achieved being the largest one in this set of experiments using POPC/POPS membranes. Reducing the  $\text{Ca}^{2+}$  concentration decreases  $\Delta f_{\text{max}}$ . The dissociation constants obtained for the three different  $\text{Ca}^{2+}$  concentrations only increase slightly by a factor of 2. Interestingly, if no  $\text{Ca}^{2+}$  was added to the solution annexin A2t binding was still discernible. The maximum frequency shift was  $-\Delta f_{\text{max}} = (25 \pm 8)$  Hz, and the corresponding dissociation constant was determined to be  $K_d = (0.59 \pm 0.26)$   $\mu\text{M}$ . Only in the presence of 0.1 mM EGTA was annexin A2t binding fully suppressed. It should be mentioned that at  $\text{Ca}^{2+}$  concentra-

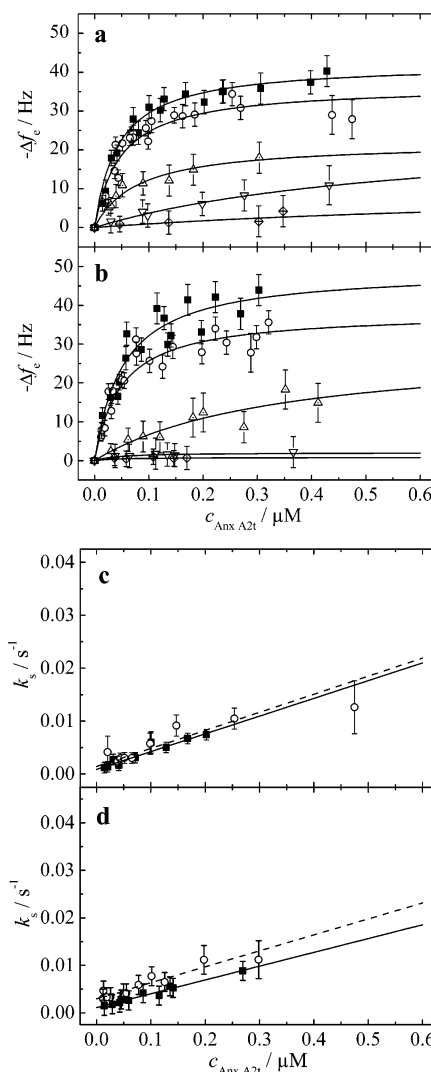


FIGURE 2: (a/b) Equilibrium frequency shifts ( $\Delta f_e$ ) as a function of protein concentration. The solid lines are the results of fitting the parameters of eq 1 to the data obtained at 1 mM  $\text{CaCl}_2$  (■), 0.1 mM  $\text{CaCl}_2$  (○), 10  $\mu\text{M}$   $\text{CaCl}_2$  (△), 0 mM  $\text{CaCl}_2$  (▽), and 0.1 mM EGTA (diamond with cross). (c/d) Time constant  $k_s$  dependent on the annexin A2t concentration. The solid line is the result of fitting the parameters of eq 3 to the data for 1 mM  $\text{CaCl}_2$  (■) and the dotted line for 0.1 mM  $\text{CaCl}_2$  (○). The solid supported membranes were composed of POPC/POPS (80:20) (a/c) and POPC/POPS/cholesterol (56:14:30) (b/d). The values for  $\Delta f_{\text{max}}$  and  $K_d$  are summarized in Table 1, those for  $k^+$  and  $k^-$  in Table 2.

tions below 10  $\mu\text{M}$  a slight drift of the frequency occurs after addition of annexin A2t to the solid supported membrane resulting in a larger error of  $\Delta f_e$ .

In previous studies, it was shown that binding of recombinant annexin A2t to liposomes containing negatively charged lipids was increased in the presence of cholesterol and that even a  $\text{Ca}^{2+}$ -independent protein binding was detected (20, 24). To obtain quantitative data of a cholesterol-induced  $\text{Ca}^{2+}$ -independent binding of annexin A2, we used solid supported bilayers composed of POPC/POPS/cholesterol (56:14:30) in the outer leaflet (Figure 2b, Table 1). It turned out that in general the same tendency for  $\Delta f_{\text{max}}$  was observed as in the case of membranes without cholesterol. Reducing the  $\text{Ca}^{2+}$  concentration leads to a decrease in  $\Delta f_{\text{max}}$ . Also, the dissociation constants were rather similar for 1 and 0.1 mM  $\text{CaCl}_2$ . Unexpectedly, for  $\text{Ca}^{2+}$  concentrations below 0.1 mM the dissociation constant increased significantly,



Table 1: Maximum Frequency Shifts and Dissociation Constants of the Interaction of Annexin A2t with Solid Supported Membranes

membrane system	$c_{\text{Ca}^{2+}}$ mM	$-\Delta f_{\text{max}}$ Hz	$K_d$ $\mu\text{M}$
POPC/POPS 80:20	1	$42 \pm 2$	$0.043 \pm 0.006$
	0.1	$37 \pm 3$	$0.048 \pm 0.009$
	0.01	$22 \pm 3$	$0.079 \pm 0.015$
	0 <sup>a</sup>	$25 \pm 8$	$0.59 \pm 0.26$
	0 <sup>b</sup>	n.b.	n.b.
POPC/POPS/chol 56:14:30	1	$49 \pm 5$	$0.053 \pm 0.015$
	0.1	$38 \pm 3$	$0.049 \pm 0.008$
	0.01	$29 \pm 9$	$0.34 \pm 0.16$
	0 <sup>a</sup>	n.b.	n.b.
	0 <sup>b</sup>	n.b.	n.b.
POPC/POPS 50:50	1	$47 \pm 2$	$0.035 \pm 0.006$
POPC/POPS 80:20	1	$42 \pm 2$	$0.043 \pm 0.006$
POPC/POPS 90:10	1	$42 \pm 3$	$0.075 \pm 0.005$
POPC/POPS 95:5	1	$50 \pm 6$	$0.20 \pm 0.05$
POPC/POPS 97:3	1	$41 \pm 11$	$0.38 \pm 0.15$
POPC	1	n.b.	n.b.
bbPC/bbPS 75:25 (w/w)	1	$42 \pm 3$	$0.079 \pm 0.013$
	0 <sup>b</sup>	n.b.	n.b.
bbPC/bbPS/chol 50:25:25 (w/w/w)	1	$45 \pm 4$	$0.081 \pm 0.013$
	0 <sup>b</sup>	n.b.	n.b.

<sup>a</sup> No  $\text{CaCl}_2$  was added to the buffer solution. <sup>b</sup> 0.1 mM EGTA was added to the buffer solution.

and no binding was detected in the absence of calcium ions. These results are in contrast to those obtained by Ayala-Sanmartin et al. (19, 23) who could show a  $\text{Ca}^{2+}$ -independent binding of annexin A2t expressed recombinantly in yeast to PC/PS/cholesterol containing liposomes. As in the case of membranes lacking cholesterol, a frequency drift occurs after addition of annexin A2t to the solid supported membranes resulting in a larger error of  $\Delta f_e$ .

If not the dissociation constant characterizing the binding affinity of annexin A2t to lipid membranes is influenced by the presence of cholesterol, it might be the kinetic behavior that is altered by cholesterol as it was observed for annexin A1 (29). To determine the rate constants of adsorption  $k^+$  and desorption  $k^-$ , we assumed that all binding sites are equal and independent of each other and that the rate-limiting step is the adsorption of the protein to the surface. Neglecting diffusion-limiting steps and excluding cooperative processes we obtain eq 2 for the binding process:

$$\Delta f(t) = \Delta f_e (1 - \exp(-k_s t)) \quad (2)$$

$k_s$  is the protein concentration-dependent rate constant defined as (eq 3):

$$k_s(c_{\text{AnnA2t}}) = k^+ c_{\text{AnnA2t}} + k^- \quad (3)$$

Rate constants  $k_s$  were obtained by fitting eq 2 to the data as described in more detail elsewhere (29) and plotted vs the annexin A2t concentration (Figure 2c,d).  $k^+$  and  $k^-$  were extracted from the plot according to eq 3. Rate constants of association and dissociation were determined for POPC/POPS (80:20) (Figure 2c) and POPC/POPS/cholesterol (56:14:30) membranes (Figure 2d) in the presence of 1 and 0.1 mM  $\text{CaCl}_2$ . The results, summarized in Table 2, clearly show that neither cholesterol nor the  $\text{Ca}^{2+}$  concentration in the range analyzed here influences the kinetics of annexin A2t binding.

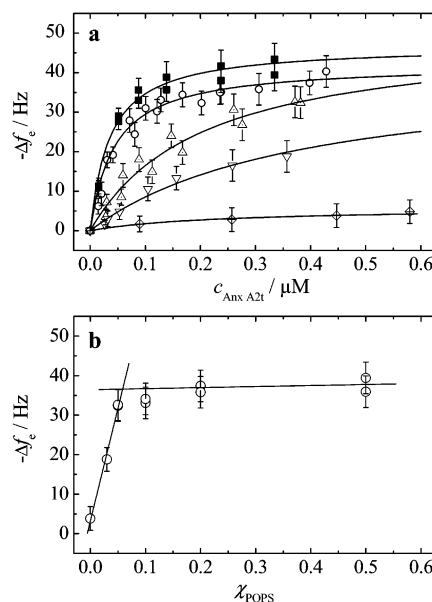


FIGURE 3: Effect of the PS content in POPC/POPS membranes on annexin A2t binding. (a) Equilibrium frequency shifts ( $\Delta f_e$ ) as deduced from different time courses as a function of protein concentration. The solid lines are the results of fitting the parameters of eq 1 to the data for 50 mol % POPS (■), 20 mol % POPS (○), 5 mol % POPS (△), 3 mol % POPS (▽) and 0 mol % POPS (diamond with cross). The values for  $\Delta f_{\text{max}}$  and  $K_d$  are summarized in Table 1. (b) Equilibrium frequency shifts ( $\Delta f_e$ ) at an annexin A2t concentration of  $0.35 \mu\text{M}$  as a function of the PS content. The intercept of the two solid lines indicates the minimum PS surface concentration required for maximum protein surface coverage.

Table 2: Summary of Rate Constants  $k^+$  and  $k^-$  Obtained from Fitting the Curves Presented in Figure 2c,d

membrane system	$c_{\text{Ca}^{2+}}$ mM	$k^+$ $10^3 \text{ M}^{-1} \text{ s}^{-1}$	$k^-$ $10^{-3} \text{ s}^{-1}$
POPC/POPS 80:20	1	$34 \pm 3$	$0.9 \pm 0.3$
	0.1	$34 \pm 6$	$1.4 \pm 0.5$
POPC/POPS/chol 56:14:30	1	$29 \pm 2$	$1.1 \pm 0.2$
	0.1	$34 \pm 5$	$3.0 \pm 0.4$

**Variation of the PS Content.** The results obtained from QCM measurements indicate that annexin A2t binds to artificial membranes in a strictly  $\text{Ca}^{2+}$ -dependent manner. It is assumed that such a  $\text{Ca}^{2+}$ -dependent binding involves simultaneous interactions of annexins,  $\text{Ca}^{2+}$  ions and PS molecules (34). By varying the PS concentration in the membrane, we elucidated the minimum amount of PS necessary for annexin A2t binding and analyzed how the PS content influences the maximum surface coverage and binding affinity of the protein. Dissociation constants for the binding of annexin A2t to POPC/POPS membranes containing 50, 20, 10, 5, 3, and 0 mol % POPS, respectively, were determined by concentration-dependent measurements in the presence of 1 mM  $\text{CaCl}_2$  (Figure 3a, binding curve for 10 mol % POPS not shown).  $\Delta f_{\text{max}}$  and  $K_d$  values obtained by fitting eq 1 to the data are summarized in Table 1. Reducing the PS surface concentration in the outer leaflet only leads to a slight decrease in  $-\Delta f_{\text{max}}$  from  $(47 \pm 2)$  Hz for POPC/POPS mixtures containing 50 mol % negatively charged lipid to  $(41 \pm 11)$  Hz for membranes containing 3 mol % POPS. However, dissociation constants increase by a factor of 10 from  $(0.035 \pm 0.006) \mu\text{M}$  for POPC/POPS (50:50) membranes to  $(0.38 \pm 0.15) \mu\text{M}$  for POPC/POPS (97:3)

membranes. Only the absence of negatively charged PS lipids prevents annexin A2t binding. To determine the required minimum PS surface concentration for maximum protein surface coverage at a protein concentration of 35  $\mu\text{M}$  the frequency shift  $-\Delta f_e$  was plotted versus the PS content (Figure 3b). The minimum PS surface concentration was obtained by two linear regressions—one in the range of 0–5 mol % PS and the other one in the saturation region. The intersection of the two lines represents the minimum PS surface concentration at maximum protein coverage, which was determined to be  $(6 \pm 1)$  mol % PS.

**Reversibility of Annexin A2t Adsorption/Desorption.** The reversibility of annexin A2t binding to solid supported membranes was analyzed by two sets of experiments: (i) The protein was first bound to the membrane in the presence of  $\text{Ca}^{2+}$  ions followed by a stepwise decrease in  $\text{Ca}^{2+}$  concentration by adding EGTA. (ii) Annexin A2t was added to an EGTA-containing solution, and membrane binding was triggered by a stepwise increase in  $\text{Ca}^{2+}$ .

In the first set of experiments, annexin A2t was bound to a solid supported membrane in the presence of 0.1 and 1 mM  $\text{CaCl}_2$ , respectively. Two different  $\text{Ca}^{2+}$  concentrations were chosen to clarify whether the reversibility of protein binding depends on the initial  $\text{Ca}^{2+}$  concentration. Annexin concentrations were ensured to be larger than 0.35  $\mu\text{M}$  to guarantee maximum surface coverage. Protein adsorption in the presence of  $\text{Ca}^{2+}$  ions leads to a frequency shift termed  $\Delta f_{\text{AnnA2t}, \text{Ca}^{2+}}$ . Adding increasing amounts of an EGTA solution resulted in a stepwise desorption of annexin A2t discernible by a stepwise increase in resonance frequency termed  $\Delta f_{\text{EGTA}}$ . A representative EGTA titration experiment is illustrated in Figure 4a. Desorption of the protein from the membrane was fast upon EGTA addition indicating that the protein–membrane complex is disrupted within seconds.

For evaluating the EGTA titration experiments, a Langmuir adsorption isotherm was not valid as the slopes of the titration curves were to some extent much larger than one indicating a cooperative process. To account for this, a Hill equation (eq 4) was used (35) considering an “interaction” coefficient  $n$  reflecting the extent of cooperativity among multiple  $\text{Ca}^{2+}$ -binding sites (31):

$$\Theta = \frac{\Delta f_{\text{AnnA2t}, \text{Ca}^{2+}} - \Delta f_{\text{EGTA}}}{\Delta f_{\text{AnnA2t}, \text{Ca}^{2+}}} = \frac{(c_{\text{Ca}^{2+}})^n}{K_d + (c_{\text{Ca}^{2+}})^n} = \frac{(c_{\text{Ca}^{2+}})^n}{(K_{0.5})^n + (c_{\text{Ca}^{2+}})^n} \quad (4)$$

The surface coverage  $\Theta$  is defined as the relative amount of binding sites occupied by annexin A2t and the total amount of binding sites present on the membrane. The denominator of eq 4 corresponds to the frequency shift obtained from the annexin A2t adsorption at a defined  $\text{Ca}^{2+}$  concentration  $\Delta f_{\text{AnnA2t}, \text{Ca}^{2+}}$ . The numerator is equal to the difference between this frequency shift and the values for  $\Delta f_{\text{EGTA}}$ , which are obtained upon addition of EGTA.  $c_{\text{Ca}^{2+}}$  represents the actual free  $\text{Ca}^{2+}$  concentration in solution, which is calculated according to Stockbridge (36) using a program written in Mathcad 2001.  $K_{0.5}$  is the  $\text{Ca}^{2+}$  concentration, at which half of the proteins are bound to the membrane, and is equivalent to the  $n$ th root of the dissociation constant  $K_d$ . This

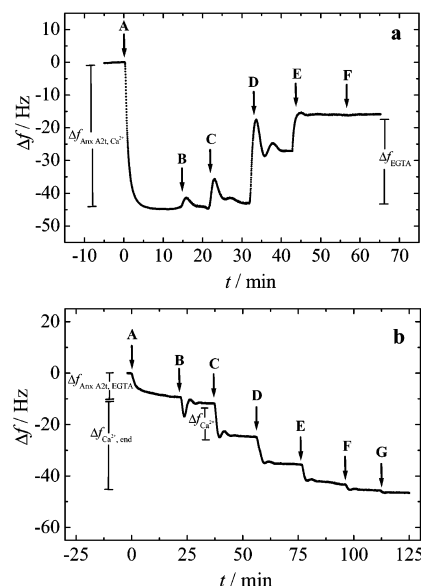


FIGURE 4: (a) Representative time course of the adsorption of 0.43  $\mu\text{M}$  annexin A2t to a POPC/POPS (80:20) membrane in the presence of 1 mM  $\text{CaCl}_2$  (A) followed by desorption due to stepwise complexation of  $\text{Ca}^{2+}$  ions by injection of EGTA solutions (20 mM Tris/HCl, 0.1 M NaCl, 1 mM  $\text{NaN}_3$ , pH 7.4 with either 5 or 50 mM EGTA) (B–F). The calculated free  $\text{Ca}^{2+}$  concentrations are (B)  $(4.1 \pm 0.3) \times 10^{-4}$  M, (C)  $(1.1 \pm 0.3) \times 10^{-4}$  M, (D)  $(2.1 \pm 0.3) \times 10^{-7}$  M, (E)  $(8.0 \pm 0.5) \times 10^{-8}$  M and (F)  $(3.6 \pm 0.5) \times 10^{-8}$  M. (b) Representative time course of the adsorption of 0.35  $\mu\text{M}$  annexin A2t to a POPC/POPS (80:20) membrane in the presence of 0.1 mM EGTA (A) followed by adsorption due to stepwise addition of  $\text{Ca}^{2+}$  (20 mM Tris/HCl, 0.1 M NaCl, 1 mM  $\text{NaN}_3$ , pH 7.4 with either 1 or 10 mM  $\text{CaCl}_2$ ) (B–G). The calculated free  $\text{Ca}^{2+}$  concentrations are (B)  $(8.0 \pm 0.3) \times 10^{-8}$  M, (C)  $(2.0 \pm 0.3) \times 10^{-7}$  M, (D)  $(2.9 \pm 0.3) \times 10^{-5}$  M, (E)  $(1.8 \pm 0.5) \times 10^{-4}$  M, (F)  $(3.9 \pm 0.5) \times 10^{-4}$  M, and (G)  $(5.8 \pm 0.5) \times 10^{-4}$  M.

simplification is necessary because such  $\text{Ca}^{2+}$  titrations arise from a complex set of equilibria so that the obtained midpoints ( $K_{0.5}$  values) do not represent single equilibrium constants. Note that the maximum amount of protein that can bind to the membrane depends on the  $\text{Ca}^{2+}$  concentration and that at 0.1 mM  $\text{CaCl}_2$  the value for  $\Delta f_{\text{AnnA2t}, \text{Ca}^{2+}}$  is smaller than at 1 mM  $\text{CaCl}_2$ .

In the second set of experiments, annexin A2t ( $>0.35 \mu\text{M}$ ) was added to solid supported membranes in the presence of 0.1 mM EGTA leading to a faint frequency shift termed  $\Delta f_{\text{AnnA2t}, \text{EGTA}}$ . A stepwise increase in the  $\text{Ca}^{2+}$  concentration resulted in a decrease in resonance frequency  $\Delta f_{\text{Ca}^{2+}}$  indicative of a stepwise protein adsorption up to a final value of  $\Delta f_{\text{Ca}^{2+}, \text{end}}$  (Figure 4b). In this case, the Hill equation is expressed in terms of  $\Delta f_{\text{AnnA2t}, \text{EGTA}}$ , which is the frequency shift upon protein addition in the presence of 0.1 mM EGTA,  $\Delta f_{\text{Ca}^{2+}}$  the shift after stepwise addition of  $\text{Ca}^{2+}$ , and  $\Delta f_{\text{Ca}^{2+}, \text{end}}$  the one at the end of the titration experiment (eq 5):

$$\Theta = \frac{\Delta f_{\text{AnnA2t}, \text{EGTA}} + \Delta f_{\text{Ca}^{2+}}}{\Delta f_{\text{AnnA2t}, \text{EGTA}} + \Delta f_{\text{Ca}^{2+}, \text{end}}} = \frac{(c_{\text{Ca}^{2+}})^n}{(K_{0.5})^n + (c_{\text{Ca}^{2+}})^n} \quad (5)$$

The reversibility of annexin A2t binding was investigated for membranes composed of POPC/POPS varying in the POPS content and for those containing a POPC/POPS (80:20) mixture with 30 mol % cholesterol. The results obtained for all membrane systems are depicted in Figure 5 together with the fitting results using eqs 4 and 5, respectively. All parameters are summarized in Table 3.

Table 3: Summary of the Fitting Parameters Obtained from the Titration Curves Presented in Figures 5 and 6c,d<sup>a</sup>

membrane system	$C_{Ca^{2+},AnxA2t}$ mM	$K_{0.5}$ nM	$n$	$\Theta'$	$K'_{0.5}$ $\mu$ M	$n'$
POPC/POPS 80:20	1	$140 \pm 20$	$4.2 \pm 1.0$	$0.87 \pm 0.07$	$70 \pm 20$	$0.9 \pm 0.5$
	0.1	$170 \pm 40$	$2.4 \pm 1.3$	$0.71 \pm 0.11$	$30 \pm 10$	$1.9 \pm 1.0$
POPC/POPS/chol 56:14:30	0 <sup>b</sup>	$230 \pm 50$	$3.3 \pm 0.9$	$0.50 \pm 0.07$	$32 \pm 6$	$1.1 \pm 0.3$
	1	$90 \pm 10$	$3.6 \pm 1.3$	$0.88 \pm 0.10$	$110 \pm 50$	$1.0 \pm 0.5$
	0.1	$210 \pm 40$	$2.9 \pm 1.7$	$0.55 \pm 0.11$	$30 \pm 6$	$1.6 \pm 0.6$
	0 <sup>b</sup>	$480 \pm 110$	$2.8 \pm 1.6$	$0.35 \pm 0.07$	$30 \pm 8$	$1.4 \pm 0.2$
POPC/POPS 50:50	1	$51 \pm 5$	$3.2 \pm 0.9$			
POPC/POPS 80:20	1	$140 \pm 20$	$4.2 \pm 1.0$	$0.87 \pm 0.07$	$70 \pm 20$	$0.9 \pm 0.5$
POPC/POPS 90:10	1	$570 \pm 130$	$1.1 \pm 0.5$	$0.66 \pm 0.14$	$370 \pm 160$	$2.3 \pm 1.1$
POPC/POPS 95:5	1	$630 \pm 150$	$1.5 \pm 0.9$	$0.52 \pm 0.23$	$220 \pm 80$	$1.9 \pm 0.9$
POPC/POPS 97:3	1				$720 \pm 120^c$	$1.8 \pm 0.8^c$
bbPC/bbPS 75:25 (w/w)	1	$110 \pm 20$	$4.1 \pm 1.6$			
	0 <sup>b</sup>	$400 \pm 190$	$2.3 \pm 1.5$	$0.39 \pm 0.08$	$50 \pm 10$	$1.3 \pm 0.3$
bbPC/bbPS/chol 50:25:25 (w/w/w)	1	$130 \pm 20$	$4.8 \pm 2.1$			
	0 <sup>b</sup>	$620 \pm 90$	$2.3 \pm 0.6$	$0.34 \pm 0.3$	$21 \pm 9$	$1.4 \pm 0.2$

<sup>a</sup>  $K_{0.5}$  and  $n$  represent the calcium ion concentrations for half maximum binding and Hill-coefficients obtained for the first inflection point.  $K'_{0.5}$  and  $n'$  are corresponding values obtained for the second inflection point. <sup>b</sup> 0.1 mM EGTA was added to the buffer solution. <sup>c</sup> These values are obtained at a protein surface coverage of only 50% compared to that obtained at higher PS contents in the membrane (see Figure 3).

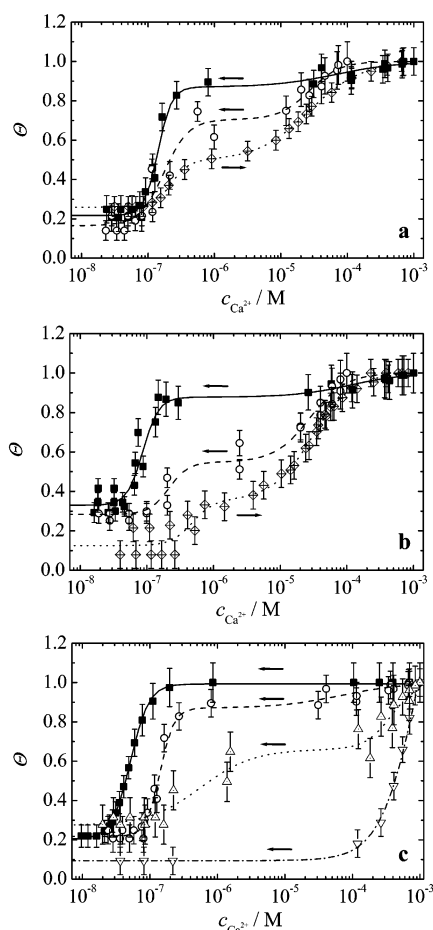


FIGURE 5:  $Ca^{2+}$ -dependent binding and desorption of annexin A2t to (a) POPC/POPS (80:20) and (b) POPC/POPS/cholesterol (56:14:30) membranes. The values for the surface coverage  $\Theta$  were obtained from the desorption of annexin A2t due to stepwise addition of EGTA (arrows pointing to the left) to solutions containing 1 mM  $CaCl_2$  (■) or 0.1 mM  $CaCl_2$  (○) or stepwise addition of  $CaCl_2$  (arrows pointing to the right) to an annexin A2t and EGTA containing solution (diamond with cross). (c)  $Ca^{2+}$ -dependent desorption of annexin A2t from POPC/POPS membranes containing 50 mol % POPS (■), 20 mol % POPS (○), 10 mol % POPS (△) and 3 mol % POPS (▽). The values for half-maximum protein binding as well as the Hill-coefficients are summarized in Table 3. The total annexin A2t concentration was  $>0.35 \mu$ M in all experiments.

The titration curves reveal two striking features. First, a significant hysteresis between the  $Ca^{2+}$ -dependent adsorption and desorption of annexin A2t occurs. Second, protein adsorption is not a single step process but takes place in two distinct steps. To a less pronounced extent, this also applies to the desorption process, however, with a strong dependency on the lipid composition.

For a POPC/POPS (80:20) membrane (Figure 5a), to which annexin A2t had been bound in the presence of 1 mM  $CaCl_2$  the first inflection point with  $K'_{0.5} = (70 \pm 20) \mu$ M and a Hill coefficient of  $n' = 0.9 \pm 0.5$  is only barely visible as most of the protein remains bound to the membrane (surface coverage  $\Theta' = 0.87 \pm 0.07$ ). The second inflection point at low  $Ca^{2+}$  concentrations is very pronounced leading to an almost complete dissociation of the annexin A2t–membrane complex with high cooperativity ( $n = 4.2 \pm 1.0$ ) and a half-maximum  $Ca^{2+}$  concentration of  $K_{0.5} = (140 \pm 20)$  nM. Around 20% of the protein remains bound to the membrane even at  $Ca^{2+}$  concentrations of less than 50 nM. Interestingly, the first desorption step is much more pronounced if annexin A2t was bound at 0.1 mM instead of 1 mM  $CaCl_2$ . Only 70% of the protein remains attached after a first protein fraction has been released from the membrane at free  $Ca^{2+}$  concentrations of 10 micromolar. The stepwise increase in  $Ca^{2+}$  ions in the presence of soluble annexin A2t leads to an association titration curve that does not match the dissociation curve. In the presence of 0.1 mM EGTA, only  $(20 \pm 10)\%$  of the protein bound to the membrane, which is, within the error of the experiment, consistent with the experiments shown in Figure 2. The following  $Ca^{2+}$ -dependent annexin A2t adsorption to POPC/POPS lipid layers occurring at  $Ca^{2+}$  concentrations in the submicromolar range is highly cooperative ( $n = 3.3 \pm 0.9$ ) and only leads to a surface coverage of approximately 50%. To obtain a full coverage higher  $Ca^{2+}$  concentrations in the micromolar range are necessary.

Similar results were obtained for POPC/POPS membranes containing 30 mol % cholesterol (Figure 5b, Table 3). One major difference to membranes without cholesterol was the lower intermediate surface coverage for desorption of annexin A2t that had been bound at 0.1 mM  $CaCl_2$  ( $\Theta' = 0.55 \pm 0.11$ ). Another difference is seen in the adsorption

experiments with increasing the  $\text{Ca}^{2+}$  concentrations. Here, only about 35% of the protein is attached to the membrane in the submicromolar range as compared to 50% in the absence of cholesterol. Furthermore, more  $\text{Ca}^{2+}$  is necessary to obtain complete surface coverage.

Figure 5c and Table 3 reveal that the intermediate surface coverage  $\Theta'$  was mostly influenced by the amount of PS in the membrane. In these experiments, annexin A2t was bound in the presence of 1 mM  $\text{CaCl}_2$  to POPC/POPS membranes with varying PS content and then released from the membrane by successive EGTA additions (Figure 5c, titration curve for 5 mol % POPS not shown). Only for POPC/POPS membranes containing 50 mol % POPS a titration curve with only one inflection point at  $K_{0.5} = (51 \pm 5)$  nM and a cooperativity coefficient of  $n = 3.2 \pm 0.9$  was observed. For membranes with a lower PS content, a second inflection point in the micromolar range emerged. Moreover, the intermediate surface coverage  $\Theta'$  is reduced from  $0.87 \pm 0.07$  for POPC/POPS (80:20) membranes to  $0.52 \pm 0.23$  for membranes containing only 5 mol % POPS. In the case of POPC/POPS (97:3) membranes, the inflection point in the submicromolar range finally disappeared and only one dissociation occurred. It should be noted that for POPC/POPS (97:3) membranes the EGTA titration experiment was actually performed at a protein surface coverage of only 50% of that obtained for POPC/POPS (50:50) membranes under the same conditions.

In summary, the results give for the first time a detailed insight into the reversibility of annexin A2t binding to lipid membranes and demonstrate that the  $\text{Ca}^{2+}$ -induced adsorption and desorption comprise several cooperative steps that are modulated by the initial bound state of the protein and the membrane composition.

**Solid Supported Membranes Composed of Bovine Brain Lipids.** The obtained results show that annexin A2t strongly interacts with solid supported membranes with high affinity. Moreover, the half-maximum  $\text{Ca}^{2+}$  concentration required for binding of at least a portion of the protein is rather low and in the submicromolar range. However, a  $\text{Ca}^{2+}$ -independent binding of annexin A2t in the presence of cholesterol as was previously described by Ayala-Sanmartin and co-workers (20, 24) using bovine brain phospholipids was not detected. As it is possible that the membrane composition chosen in our experiments might be the reason for the lack of a  $\text{Ca}^{2+}$ -independent binding, we performed quartz crystal microbalance experiments with membranes composed of the lipid mixtures used by Ayala-Sanmartin and co-workers, namely, bbPC/bbPS 75:25 (w/w) and bbPC/bbPS/cholesterol 50:25:25 (w/w/w) (20, 24). By concentration-dependent measurements, dissociation constants of annexin A2t to these membranes were determined in the presence of 1 mM  $\text{CaCl}_2$  and 0.1 mM EGTA (Figure 6a,b). The results are similar to those obtained for POPC/POPS mixtures and the values obtained for the maximum frequency shifts  $\Delta f_{\text{max}}$  and the dissociation constants  $K_d$  are summarized in Table 1. Again no annexin A2t binding was detected in the absence of  $\text{Ca}^{2+}$  and the addition of cholesterol to the lipid mixture did not alter the binding affinity and maximum frequency shift, respectively, nor did it induce a  $\text{Ca}^{2+}$ -independent binding of annexin A2t to cholesterol containing membranes. It is, however, noteworthy that even though the  $\Delta f_{\text{max}}$  values are

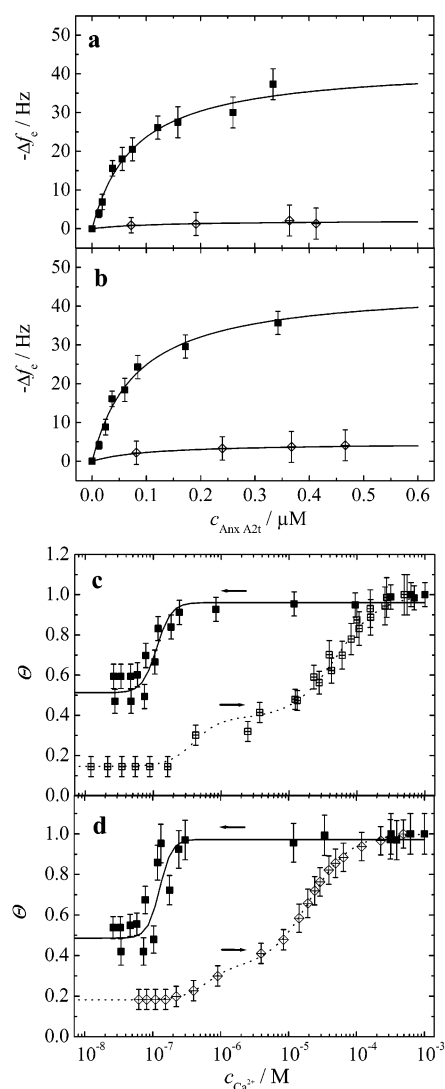


FIGURE 6: (a/b) Equilibrium frequency shifts ( $\Delta f_e$ ) as deduced from different time courses as a function of protein concentration. The solid lines are the results of fitting the parameters of eq 1 to the data for 1 mM  $\text{CaCl}_2$  (■) and 0.1 mM EGTA (diamond with cross). (c/d)  $\text{Ca}^{2+}$ -dependent binding and desorption of annexin A2t. The values for the surface coverage  $\Theta$  were obtained from the desorption of annexin A2t due to stepwise addition of EGTA (arrows pointing to the left) to solutions containing 1 mM  $\text{CaCl}_2$  (■). In a reverse experiment, annexin A2t was added to the membranes in the presence of EGTA (diamond with cross). Increasing amounts of  $\text{Ca}^{2+}$  (arrows pointing to the right) were added to induce a  $\text{Ca}^{2+}$ -dependent binding of the protein. The total annexin A2t concentration was  $>0.35 \mu\text{M}$  in all experiments. The solid supported membranes were composed of bbPC/bbPS 75:25 (w/w) (a/c) and bbPC/bbPS/cholesterol 50:25:25 (w/w/w) (b/d). The values for  $\Delta f_{\text{max}}$  and  $K_d$  are summarized in Table 1, and those for half-maximum protein binding, the Hill coefficients, and intermediate surface coverages are summarized in Table 3.

in the same range as those obtained for POPC/POPS (80:20) mixtures found in the presence of 1 mM  $\text{CaCl}_2$  the dissociation constants are increased by a factor of 2.

Titration experiments as those described for POPC/POPS mixtures were performed to verify the reversibility of membrane binding (Figure 6c,d, Table 3). In contrast to the results obtained for POPC/POPS membranes, A2t desorption from bbPC/bbPS 75:25 (w/w) occurred in one single step at an inflection point of  $(110 \pm 20)$  nM with high cooperativity ( $n = 4.1 \pm 1.6$ ). Moreover, only about 50% of the bound



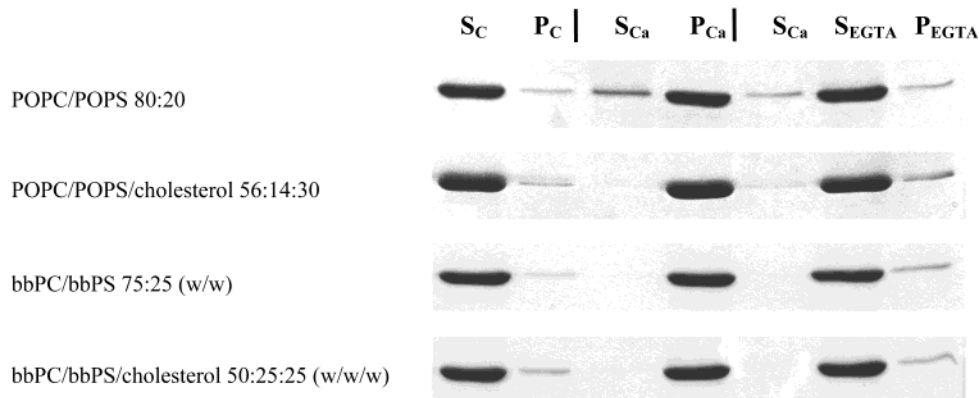


FIGURE 7: Annexin A2t binding to liposomes. Identical amounts of annexin A2t were incubated with POPC/POPS, POPC/POPS/cholesterol, bbPC/bbPS, and bbPC/bbPS/cholesterol liposomes in the presence of 1 mM  $\text{CaCl}_2$ . After centrifugation of the sample, supernatants and pellets were analyzed by SDS-PAGE ( $S_{\text{Ca}}$  and  $P_{\text{Ca}}$ ). In experiments analyzing the reversibility of membrane binding membrane bound protein was released with excess of EGTA. After incubation, the mixtures were centrifuged and analyzed by SDS-PAGE ( $S_{\text{EGTA}}$  and  $P_{\text{EGTA}}$ ) and compared to a liposome-free control ( $S_{\text{C}}$  and  $P_{\text{C}}$ ). The figures shown are representative for two different experiments.

protein was reversibly detached by the addition of EGTA compared to POPC/POPS membranes, where almost 80% of bound annexin A2t was removed by addition of EGTA. The presence of cholesterol did not alter the desorption behavior of annexin A2t. For the calcium-induced adsorption again two binding processes at different characteristic  $\text{Ca}^{2+}$  concentrations were monitored.

**Binding of Annexin A2t to Liposomes.** It is conceivable that the protein fraction, which binds  $\text{Ca}^{2+}$  independently to solid supported membranes, is bound to defects in the membrane due to nonspecific hydrophobic interactions. It is also possible that reduced lipid diffusion within a solid supported membrane influences the  $\text{Ca}^{2+}$  dependency of annexin A2t binding. To elucidate this, we compared our results obtained for solid supported membranes with those typically obtained in conventional liposome binding experiments. Liposome copelleting assays have been used widely in the past to characterize annexin binding to membranes and to determine  $\text{Ca}^{2+}$  concentrations for half-maximum membrane binding (15, 16, 20, 22–24).

Binding of annexin A2t to liposomes was studied by incubating identical amounts of annexin A2t with liposomes of POPC/POPS, POPC/POPS/cholesterol, bbPC/bbPS, and bbPC/bbPS/cholesterol in the presence of 1 mM  $\text{CaCl}_2$ . After centrifugation, supernatant, and pellets were analyzed by SDS-PAGE (Figure 7,  $S_{\text{Ca}}$  and  $P_{\text{Ca}}$ ). In all cases, 100% of the protein added to the reaction mixture bound to the liposomes. Experiments in which the reversibility of membrane binding was investigated by releasing membrane bound protein with an excess of EGTA demonstrated that removal of  $\text{Ca}^{2+}$  from solution results in an almost complete protein desorption from the liposomes. These results confirm that annexin A2t binding to liposomes is strictly  $\text{Ca}^{2+}$ -dependent (Figure 7,  $S_{\text{EGTA}}$  and  $P_{\text{EGTA}}$ ), fully reversible, and independent of membrane cholesterol and essentially reflect the results obtained by QCM measurements.

## DISCUSSION

The interaction of annexins with lipid membranes is a complex interplay between the protein,  $\text{Ca}^{2+}$  ions, and lipids. Hence, even in reduced biophysical systems binding affinity is influenced by the concentrations of all three parameters. To gain information about the influence of these compounds

on binding affinity and kinetics of annexin A2t adsorption to lipid membranes as well as the reversibility of the adsorption/desorption process, we performed quartz crystal microbalance studies using solid supported membranes. Two main questions were addressed. First, the influence of cholesterol on binding affinity and kinetics was investigated by varying the annexin A2t concentration at different lipid mixtures, while the  $\text{Ca}^{2+}$  concentration was kept constant. Second, the reversibility of annexin A2t adsorption and desorption was followed by varying the  $\text{Ca}^{2+}$  concentration and keeping the annexin A2t concentration fixed.

It is described that annexin A2t can interact with cellular membrane fractions in the absence of  $\text{Ca}^{2+}$  (37–40) and that  $\text{Ca}^{2+}$ -independently bound protein can only be released by treatment with cholesterol sequestering agents (40). This has led to the assumption that such  $\text{Ca}^{2+}$ -independent binding of annexin A2t is due to the presence of cholesterol itself, a receptor that is embedded into a cholesterol-rich domain of the membrane (39) or a specific membrane structure (41). To investigate the influence of cholesterol itself in our *in vitro* system, we monitored adsorption isotherms and protein-dependent rate constants as a function of the  $\text{Ca}^{2+}$  concentration and cholesterol content in the membrane. In contrast to an expected  $\text{Ca}^{2+}$ -independent binding, the binding affinity decreased considerably with decreasing  $\text{Ca}^{2+}$  concentrations. In the presence of cholesterol already a decrease to 10  $\mu\text{M}$   $\text{CaCl}_2$  was sufficient to prevent annexin A2t binding, a concentration that is still high enough for annexin A2t membrane binding in the absence of cholesterol. To confirm our QCM observations we performed liposome binding assays, which also indicated that annexin A2t does not bind in a  $\text{Ca}^{2+}$ -independent manner to cholesterol-containing membranes. These results disagree with those obtained by Ayala-Sanmartin and co-workers (20, 24) describing a  $\text{Ca}^{2+}$ -independent binding of annexin A2t to bbPC/bbPS/cholesterol containing liposomes. In contrast to our experiments employing annexin A2t purified from porcine intestine Ayala-Sanmartin and co-workers used recombinant annexin A2 generated in a yeast expression system, which was subsequently mixed with p11 to form the heterotetramer complex. At present it is unclear, whether the protein source might affect the binding properties of the protein. On the basis of our results, we conclude that cholesterol is probably



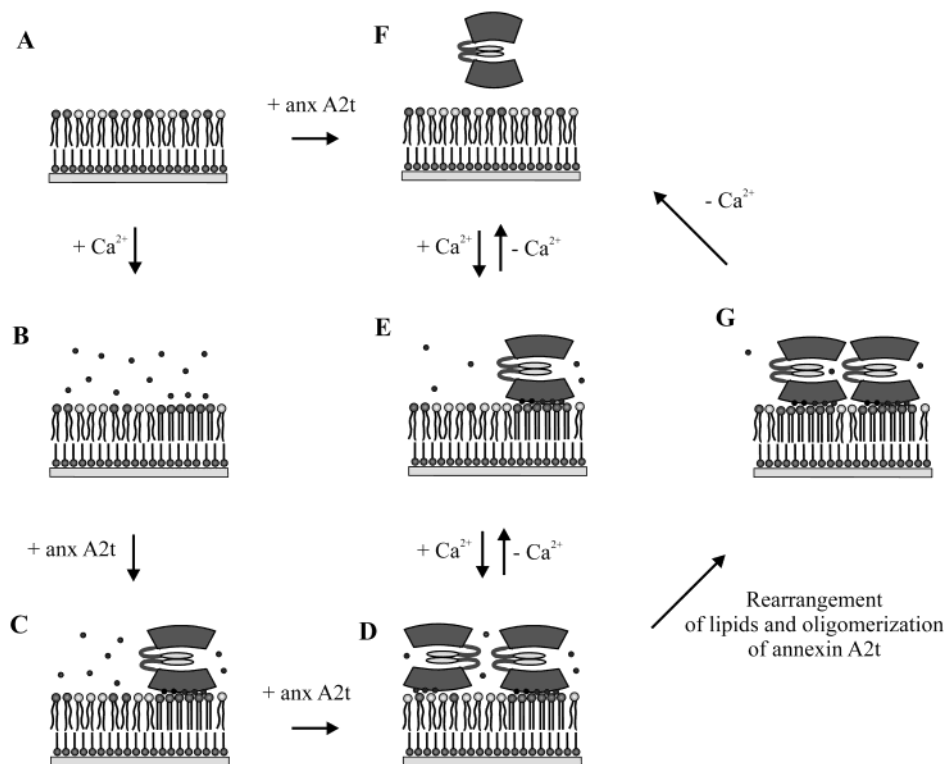


FIGURE 8: Possible scenarios of the interaction of annexin A2t with lipid membranes. A solid supported membrane composed of octanethiol chemisorbed on gold with a physisorbed lipid layer before (A) and after (B)  $\text{Ca}^{2+}$  addition is shown. Addition of annexin A2t leads to adsorption to high affinity binding (C) and low affinity binding sites (D). Noncooperative desorption from low affinity binding sites (D–E) and cooperative desorption from high affinity binding sites (E–F, G–F) occurs upon decreasing the  $\text{Ca}^{2+}$  concentration. Rearrangement of lipids and oligomerization of annexin A2t can take place at high  $\text{Ca}^{2+}$  and/or PS content (D–G). After rearrangement, desorption occurs in one step and is highly cooperative.

not the only component, which triggers the  $\text{Ca}^{2+}$ -independent binding found *in vivo*. It is more likely that a receptor embedded in a cholesterol-rich membrane domain (39) or a specific membrane structure (41) formed due to the presence of cholesterol leads to the specific localization of annexin A2t at cholesterol-rich membranes *in vivo*.

Even if the dissociation constant representing the binding affinity of annexin A2t to lipid membranes is not influenced by the presence of cholesterol, it is, however, still conceivable that the kinetic behavior is altered by cholesterol as it was observed for annexin A1 (29). However, and in contrast to the membrane interaction of annexin A1 the rate constants for annexin A2t binding were independent of the membrane composition and  $\text{Ca}^{2+}$  concentration in solution. In the case of annexin A1, the cholesterol-induced difference in rate constants was discussed in terms of a larger flexibility of the protein at lower  $\text{Ca}^{2+}$  concentrations (29). We assume that, in contrast to annexin A1, the heterotetrameric complex of annexin A2 and p11 exhibits a rather rigid structure and therefore does not show this difference. This assumption is supported by the fact that  $\text{Ca}^{2+}$  does not alter the overall secondary structure of the protein (12). In addition, the flexibility of domains is decreased in the presence of  $\text{Ca}^{2+}$  and is not further altered in the presence of phospholipids (18).

To elucidate the minimum amount of PS required for complete protein coverage at a certain protein concentration, we monitored adsorption isotherms dependent on the PS content in the outer leaflet of the membrane. A minimum amount of only 6% PS was necessary to obtain full coverage as deduced from the shift in frequency at constant protein

concentration. As the frequency shift depends on various factors a direct translation of a frequency shift into surface coverage is sometimes questionable. We assume, however, that this translation is valid under the conditions we have chosen, as the maximum frequency shifts depend not only on the  $\text{Ca}^{2+}$  concentration in solution but also on the PS content in the membrane reflecting the same tendency that is known from literature (annexin A1: (29); annexin A2: (17); annexin A5 and A6: (34)).

Although we were not able to detect a cholesterol-dependent association of annexin A2t with membranes, we intended to elucidate whether the reversibility of protein binding was influenced by the membrane composition. Dependent on the  $\text{Ca}^{2+}$  concentration in solution we investigated the reversibility of annexin A2t adsorption/desorption, while keeping the annexin A2t concentration constant, an experiment, which resembles the situation in the cell better than changing the annexin A2t concentration and keeping the  $\text{Ca}^{2+}$  concentration constant. To simplify the situation, an annexin A2t concentration was chosen leading to maximum protein binding (except for POPC/POPS (97:3) membranes). Interestingly, a hysteresis between adsorption and desorption was observed, which clearly depends on membrane composition and the initial  $\text{Ca}^{2+}$  concentration used to induce annexin A2t binding. We conclude from these results that annexin A2t can either bind to a high affinity binding site described by a cluster of PS molecules (Figure 8C) or a low affinity binding site described by single PS molecules embedded in a PC matrix (Figure 8D). Apparently, these two binding sites cannot be distinguished when increasing the annexin A2t concentration stepwise at a

constant  $\text{Ca}^{2+}$  concentration as indicated by the Langmuir-like adsorption isotherms (see Figure 2).

For the desorption process starting from protein bound at 1 mM  $\text{CaCl}_2$ , a titration curve with one sharp inflection point in the submicromolar range was discernible for bbPC/PS, bbPC/PS/cholesterol and POPC/POPS (50:50). Protein desorption in the submicromolar range is highly cooperative with a Hill coefficient of 3–5 and a low half-maximum  $\text{Ca}^{2+}$  concentration of 50–150 nM. We hypothesize that if the protein is bound to the membrane interface at high  $\text{Ca}^{2+}$  concentrations occupying high and low affinity binding sites, a lipid rearrangement underneath the protein can occur encircling small patches of phospholipid containing 28–30 PS molecules (22). Moreover, bound proteins can then laterally interact with each other (oligomerization) (Figure 8G). This process would be favored in the case of laterally mobile lipids and at high concentrations of PS and  $\text{Ca}^{2+}$  but cannot be detected by the QCM technique as no mass changes occur at the membrane/water interface. Removing the protein from the surface includes breaking off all interaction sites not only between annexin A2t and the PS molecules but also those within the protein network (Figure 8F). This would only occur at low  $\text{Ca}^{2+}$  concentrations in concert with high cooperativity and is consistent with our observations.

For POPC/POPS mixtures with a reduced PS content and for protein bound at 0.1 mM  $\text{CaCl}_2$ , we observed a second inflection point in the micromolar range. At a PS content of 3 mol % desorption in the submicromolar range was even not observable. Following our model, this implies that dependent on the PS content and the initial  $\text{Ca}^{2+}$  concentration, a second annexin A2t population is bound to low affinity binding sites on the membrane and is only loosely attached to the protein network. A similar assumption was made for annexin A5 analyzed by means of surface plasmon resonance suggesting that annexin A5 is only loosely bound to the protein network (42). In our model, the formation of stable annexin A2t–lipid complexes is, however, related to the membrane structure, which is determined by the availability of  $\text{Ca}^{2+}$  ions and PS molecules. According to Montaville and co-workers, binding of annexins to PS-containing membranes involves at least two  $\text{Ca}^{2+}$  ions and two PS molecules acting cooperatively (42). If either the  $\text{Ca}^{2+}$  concentration or the PS content is reduced an ideal formation of the ligand sphere around the  $\text{Ca}^{2+}$  ion is not possible. Thus, the protein population bound to low affinity binding sites (Figure 8D) would be already released at higher  $\text{Ca}^{2+}$  concentrations in the micromolar range without any cooperativity (Figure 8E) in line with our results.

A very interesting result is the fact that a hysteresis of the  $\text{Ca}^{2+}$  titration curves is observed. For the adsorption of annexin A2t, a two-step process is always discernible. Independent of the lipid composition, the first binding process is characterized by a low half-maximum  $\text{Ca}^{2+}$  concentration in the submicromolar range with a cooperativity of 2.3–3.3, while the second point of inflection occurs at a half-maximum  $\text{Ca}^{2+}$  concentration in the micromolar range. Following the scenario described above, it is assumed that high and low affinity binding sites are present in the membrane, but that their ratio depends on the lipid composition. Due to the high fluidity in case of POPC/POPS membranes a large number of high affinity binding sites are

immediately formed as a result of an increase in  $\text{Ca}^{2+}$  concentration in concert with annexin A2t (Figure 8F/E). As it is suggested that membrane-bound annexin induces the rearrangement of negatively charged lipids a depletion of PS molecules from the protein-free membrane fraction would result. Consequently, if all high affinity binding sites are occupied, annexin A2t can only bind to low affinity binding sites triggered at a higher  $\text{Ca}^{2+}$  concentration (Figure 8E/D). If the lateral mobility of the lipids is reduced the number of high affinity binding sites is diminished and hence less protein is bound at low  $\text{Ca}^{2+}$  concentrations. This might be the case for POPC/POPS/cholesterol, bbPC/bbPS, and bbPC/bbPS/cholesterol lipid mixtures. In this respect, it is noteworthy that in line with the existing literature our experiments were performed at room temperature and that lateral mobility of the lipids and thus the number of high affinity binding sites can be affected by increasing the temperature to 37 °C met in vivo. Other factors possibly affecting the binding of annexin A2t to cellular membranes will also come into play in vivo. These include a possible role of the cortical cytoskeleton in stabilizing the interaction of annexin A2t with the plasma membrane (43–48). However, such factors are at present too complex to be incorporated in our QCM studies.

Notably, an irreversibly bound portion of protein remained at the membrane in the absence of  $\text{Ca}^{2+}$ . In the case of POPC/POPS and POPC/POPS/cholesterol membranes, this amount is in the range of 10–30%, and is even higher in the case of bbPC/bbPS and bbPC/bbPS/cholesterol. In the liposome copelleting assay, no irreversibly bound protein was detected. The reason for this might be found in reduced lateral lipid mobility on the solid support and a lateral aggregation of the protein adsorbed on the planar surface. Similar results were obtained for annexin A5 bound to solid supported bilayers with surface plasmon resonance and attributed to an incomplete disruption of the formed annexin network (42).

## CONCLUSION

The quartz crystal microbalance technique enabled us to quantify the binding affinities and kinetics of the interaction between the heterotetrameric annexin A2-p11 complex and solid supported membranes with various lipid compositions as well as the reversibility of the adsorption/desorption process. The strictly  $\text{Ca}^{2+}$ -dependent adsorption of annexin A2t in the presence of cholesterol indicates that not cholesterol itself but rather a cholesterol-associated receptor or cholesterol-induced membrane domains recruit the protein to cholesterol-rich domains in the cell. The hysteresis of the adsorption/desorption process as well as the fact that two bound annexin A2t populations can be distinguished dependent on the membrane-composition point in the direction of a more modular response of annexin A2t to changes in the  $\text{Ca}^{2+}$  concentration. Once annexin A2t is bound to a membrane, the  $\text{Ca}^{2+}$  level needs to be very low to induce full desorption of the protein.

## ACKNOWLEDGMENT

We would like to thank H.-J. Galla (Institut für Biochemie, Westfälische Wilhelms-Universität Münster) for his generous support.

## REFERENCES

1. Raynal, P., and Pollard, H. B. (1994) *Biochim. Biophys. Acta* 1197, 63–93.

2. Gerke, V., and Moss, S. E. (2002) *Physiol. Rev.* 82, 331–371.
3. Pollard, H. B., and Rojas, E. (1988) *Proc. Natl. Acad. Sci. U.S.A.* 85, 2974–2978.
4. Creutz, C. E. (1992) *Science* 258, 924–931.
5. Berendes, R., Voges, D., Demange, P., Huber, R., and Burger, A. (1993) *Science* 262, 427–430.
6. Waisman, D. M. (1995) *Mol. Cell. Biochem.* 149–150, 301–322.
7. Huber, R., Schneider, M., Mayr, I., Romisch, J., and Paques, E. P. (1990) *FEBS Lett.* 275, 15–21.
8. Weng, X., Luecke, H., Song, I. S., Kang, D. S., Kim, S. H., and Huber, R. (1993) *Protein Sci.* 2, 448–458.
9. Jost, M., Thiel, C., Weber, K., and Gerke, V. (1992) *Eur. J. Biochem.* 207, 923–930.
10. Jost, M., Weber, K., and Gerke, V. (1994) *Biochem. J.* 298, 553–559.
11. Pigault, C., Follenius-Wund, A., Lux, B., and Gerard, D. (1990) *Biochim. Biophys. Acta* 1037, 106–114.
12. Gerke, V., and Weber, K. (1985) *J. Biol. Chem.* 260, 1688–1695.
13. Marriott, G., Kirk, W. R., Johnsson, N., and Weber, K. (1990) *Biochemistry* 29, 7004–7011.
14. Thiel, C., Weber, K., and Gerke, V. (1991) *J. Biol. Chem.* 266, 14732–14739.
15. Glenney, J. (1986) *J. Biol. Chem.* 261, 7247–7252.
16. Powell, M. A., and Glenney, J. R. (1987) *Biochem. J.* 247, 321–328.
17. Evans, T. C., Jr., and Nelsestuen, G. L. (1994) *Biochemistry* 33, 13231–13238.
18. Ayala-Sanmartin, J., Vincent, M., Sopkova, J., and Gally, J. (2000) *Biochemistry* 39, 15179–15189.
19. Blackwood, R. A., and Ernst, J. D. (1990) *Biochem. J.* 266, 195–200.
20. Ayala-Sanmartin, J., Henry, J. P., and Pradel, L. A. (2001) *Biochim. Biophys. Acta* 1510, 18–28.
21. Drust, D. S., and Creutz, C. E. (1988) *Nature* 331, 88–91.
22. Regnouf, F., Sagot, I., Delouche, B., Devilliers, G., Cartaud, J., Henry, J. P., and Pradel, L. A. (1995) *J. Biol. Chem.* 270, 27143–27150.
23. Filipenko, N. R., Kang, H. M., and Waisman, D. M. (2000) *J. Biol. Chem.* 275, 38877–38884.
24. Ayala-Sanmartin, J. (2001) *Biochem. Biophys. Res. Commun.* 283, 72–79.
25. Janshoff, A., Galla, H.-J., and Steinem, C. (2000) *Angew. Chem., Int. Ed.* 39, 4004–4032.
26. Janshoff, A., and Steinem, C. (2001) *Sensors Update* 9, 313–354.
27. Sauerbrey, G. (1959) *Z. Phys.* 155, 206–212.
28. Gerke, V., and Weber, K. (1984) *EMBO J.* 3, 227–233.
29. Kastl, K., Ross, M., Gerke, V., and Steinem, C. (2002) *Biochemistry* 41, 10087–10094.
30. Janshoff, A., Steinem, C., Sieber, M., el Baya, A., Schmidt, M. A., and Galla, H. J. (1997) *Eur. Biophys. J.* 26, 261–270.
31. Weiss, J. N. (1997) *FASEB J.* 11, 835–841.
32. Cutsforth, G. A., Whitaker, R. N., Hermans, J., and Lentz, B. R. (1989) *Biochemistry* 28, 7459–7461.
33. Junker, M., and Creutz, C. E. (1994) *Biochemistry* 33, 8930–8940.
34. Bazzi, M. D., and Nelsestuen, G. L. (1991) *Biochemistry* 30, 7970–7977.
35. Luo, Q., and Andrade, J. D. (1998) *J. Coll. Interface Sci.* 200, 104–113.
36. Stockbridge, N. (1987) *Comput. Biol. Med.* 17, 299–304.
37. Drust, D. S., and Creutz, C. E. (1991) *J. Neurochem.* 56, 469–478.
38. Raynal, P., Pollard, H. B., Cushman, S. W., and Guerre-Millo, M. (1996) *Biochem. Biophys. Res. Commun.* 225, 116–121.
39. Jost, M., Zeuschner, D., Seemann, J., Weber, K., and Gerke, V. (1997) *J. Cell. Sci.* 110, 221–228.
40. Harder, T., Kellner, R., Parton, R. G., and Gruenberg, J. (1997) *Mol. Biol. Cell* 8, 533–545.
41. Zeuschner, D., Stoorvogel, W., and Gerke, V. (2001) *Eur. J. Cell Biol.* 80, 499–507.
42. Montaville, P., Neumann, J. M., Russo-Marie, F., Ochsenbein, F., and Sanson, A. (2002) *J. Biol. Chem.* 277, 24684–24693.
43. Glenney, J. R., Jr., Tack, B., and Powell, M. A. (1987) *J. Cell Biol.* 104, 503–511.
44. Zokas, L., and Glenney, J. R., Jr. (1987) *J. Cell Biol.* 105, 2111–2121.
45. Harder, T., and Gerke, V. (1994) *Biochim. Biophys. Acta* 1223, 375–382.
46. Oliferenko, S., Paiha, K., Harder, T., Gerke, V., Schwärzler, C., Schwarz, H., Beug, H., Günthert, U., and Huber, L. A. (1999) *J. Cell Biol.* 146, 843–854.
47. Filipenko, N. R., and Waisman, D. M. (2001) *J. Biol. Chem.* 276, 5310–5315.
48. Thiel, C., Osborn, M., and Gerke, V. (1992) *J. Cell. Sci.* 103, 733–742.

BI027069Z